Probabilistic Seismic Hazard Analysis of Sitamarhi near Bihar-Nepal Region

Abhik Paul
Indian Institute of Technology Patna
Pradipta Chakrabortty (pradipt@gmail.com)
Indian Institute of Technology Patna https://orcid.org/0000-0002-8852-2596
Avijit Burman
National Institute of Technology Patna
Sapan Kumar
National Institute of Technology Patna

Research Article

Keywords: Seismic hazard analysis, Spectral acceleration, Peak ground acceleration, Uniform hazard spectrum, Gutenberg-Richter recurrence law

Posted Date: May 18th, 2021

DOI: https://doi.org/10.21203/rs.3.rs-475275/v1

Probabilistic Seismic Hazard Analysis of Sitamarhi near Bihar-Nepal Region

Author
Name: Mr Abhik Paul
Organization: Indian Institute of Technology Patna, India
Address: DCEE, IIT Patna, Bihta, Patna, Bihar, India-801106
Phone: +919733867894
ORCID ID- https://orcid.org/0000-0002-3759-4231
E-mail: abhik_1921ce04@iitp.ac.in

Corresponding Author
Name: Dr Pradipta Chakrabortty
Organization: Indian Institute of Technology Patna, India
Address: DCEE, IIT Patna, Bihta, Patna, Bihar, India-801106
Phone: +919470648103
ORCID ID- https://orcid.org/0000-0002-8852-2596
E-mail: pradipt@iitp.ac.in

Author
Name: Dr A. Burman
Organization: National Institute of Technology Patna, India
Address: DCE, NIT Patna, Patna, Bihar, India-800001
Phone: 91-7319829357
E-mail: avijitburman@yahoo.com; avijit@nitp.ac.in

Author
Name: Mr Sapan Kumar
Organization: National Institute of Technology Patna, India
Address: DCE, NIT Patna, Patna, Bihar, India-800005
Phone: 91-9801628081
E-mail: sapank9981@gmail.com

Abstract:

This article presents the results of a probabilistic seismic hazard analysis (PSHA) for Sitamarhi, Bihar considering the region-specific maximum magnitude and ground motion prediction equation (GMPEs). North Bihar region is one of the seismically unstable areas in India facing several destructive earthquakes for the Himalayan Mountains that was created by the collision of Indian and Eurasian plate. The Gutenberg-Richter (G-R) seismic hazard parameter 'a' and 'b' have been evaluated by considering the available local earthquake data. Earthquake data were collected from the United States geological survey (USGS), Indian Meteorological Department (IMD), New Delhi, Seismotectonic Atlas of India (GIS 2000) within 500 km radius of the study area, and 62 seismotectonic sources were identified and considered in this study. Seismic source zones for the region have been defined based on large-scale geological features, which are used for assigning the maximum possible earthquake potential. Estimated PGA values are 0.89 g and 0.61 g for the 2% and 10% probabilities of exceedance in 50 years. The results showed that West Patna fault and Sitamarhi Fault are the two main faults, which contribute maximum in the peak ground acceleration (PGA) values for Sitamarhi region.

Keyword: Seismic hazard analysis, Spectral acceleration, Peak ground acceleration, Uniform hazard spectrum, Gutenberg-Richter recurrence law

List of abbreviations:

a, b	Seismic hazard parameter
$a_1, a_2, a_3, a_4, a_m, a_7$	Regression coefficients
DSHA	Deterministic seismic hazard analysis
F_E, F_p, F_S	Period-dependent function for sources
b_1, b_2, b_3, b_4	Coefficient to be determined from regression
$f_n(m)$	Probability density function for the minimum magnitude
$f_n(r\|m)$	Conditional probability density function
GMPE	Ground motion prediction equation
IMD	Indian meteorological department
L	Rapture length
$M, mech, R_{JB}$	Predictor variables
M_b	Body wave magnitude
M_{max}	Maximum earthquake magnitude
M_0	Minimum magnitude

M_S	Surface wave magnitude
Mw	Seismic moment magnitude
$M_{W\ max}$	Maximum seismic moment magnitude
N	Cumulative no of earthquakes per year with equal or larger magnitude
$N_n(m_o)$	Earthquake frequency of seismic source
NF	Normal fault
NGA	Next generation attenuation
PDF	Probability density function
PGA	Peak ground acceleration
PSHA	Probabilistic seismic hazard analysis
R	Epicentral distance
RF	Reverse fault
SA	Spectral acceleration
SF	Slip fault
SMA	Strong motion accelerograph
SSA	Seismic study area
SSR	Structural response recorder
T	Time period
UHS	Uniform hazard spectra
USGS	United States geological survey
V_{S30}	Average seismic shear-wave velocity from the surface to a depth of 30 meters
$v(z)$	Average frequency
Y	Peak ground acceleration
λ_m	Mean annual rate of exceedance of magnitude m
σ	Standard deviation
ϵ_n	Fractional number of the standard deviations of a single predicted value of lnY away from the mean

1. Introduction

India faces several threats from various natural hazards such as flood, drought, landslide, cyclone, earthquake, tsunami etc. Earthquake is one of the most serious devastating natural hazards which occur beneath the ground

surface and release a huge amount of energy. It causes extensive damage like the collapse of the structure, massive loss of life, triggering a fire, landslides or tsunami. High seismic activity in India (Fig. 1) is clearly evident from the recent major earthquakes, i.e., Nepal earthquake in 2015, (M_w=7.5); Sikkim earthquake in 2011 (M_w=6.7); Kashmir Earthquake in 2005 (M_w=7.6); Bhuj earthquake in 2001 (M_w=7.7); Latur earthquake in 1993 (M_w=6.2). The presence of high seismic strain gap in the Himalayan region has been documented by Kumar et al. (2013a), which may cause more devastating earthquakes in the near future. The Himalayan subduction zone is the second most seismically active zone after the San Andreas Fault in the world where the earthquakes are caused due to the thrust faulting, and the earthquake focal depths vary from shallow to about 200 km. Due to the ever-increasing demand for structural growth fuelled by increasing population near Himalayan belt and Indo-Gangetic Basin, the need for seismic hazard analysis; estimation of the peak ground acceleration and the site-specific response spectra have gained importance for designing buildings, infrastructure projects as well as disaster planning and management.

Seismic hazard analysis is very important for the safe construction of seismic resistance structure. Based on regional seismological and geological evidence, the seismic hazard analysis can be evaluated using two methods: Deterministic seismic hazard analysis (DSHA) and Probabilistic seismic hazard analysis (PSHA). Burnwal et al. (2017) documented deterministic seismic hazard analysis (DSHA) and presented the peak ground acceleration (PGA) values for the Sitamarhi area near the Bihar-Nepal region. The DSHA considers just one maximum magnitude and distance scenario (Bommer and Abrahamson 2006), but the seismic hazard at a site is influenced by all the seismic sources with different magnitudes and distances. The widely used approach to estimate seismic-design loads for engineering projects is probabilistic seismic-hazard analysis (PSHA). The PSHA consists of four steps (Reiter 1990): i) identification and characterization of earthquake sources contributing to the seismic hazard of a study area, ii) seismicity or temporal distribution of earthquake recurrence must be characterized using suitable recurrence relationship, iii) use of suitable attenuation relationships to predict the distribution of ground motion intensities, and iv) the uncertainty in earthquake location, earthquake size and ground motion parameter prediction are combined to obtained the probability that the ground motion parameter (e.g., PGA) will be exceeded during a particular time period. The primary output from PSHA is the hazard curve showing the variation of selected ground-motion parameters, such as peak ground acceleration (PGA) or spectral acceleration (SA), against the annual frequency of exceedance (or its reciprocal, return period). The design value is the ground-motion level that corresponds to a pre-selected design return period (Bommer and Abrahamson 2006). PSHA can reflect the actual hazard level due to bigger

earthquakes along with smaller events, which are also crucial in the hazard estimation, due to their higher occurrence rates (Das et al. 2006). PSHA is able to correctly reflect the actual knowledge of seismicity (Orozova and Suhadolc 1999) and calculates the rate at which different levels of ground motion are exceeded at the site by considering the effects of all possible combinations of magnitude-distance scenarios. In the probabilistic approach, effects of all the earthquakes expected to occur at various locations during a specified life period are considered along with associated uncertainties and randomness of earthquake occurrences and attenuation of seismic waves with distance. Also, PSHA produces uniform hazard spectrum (UHS), which is a convenient tool to compare the hazard representations of different sites (Trifunac 1990; Todorovska et al. 1995; Peruzza et al. 2000; and Du and Pan 2020).

Joshi and Mohan (2011) developed the seismic hazard maps for the north-east Himalaya using the methodology suggested by Joshi and Patel (1997). Anbazhagan et al. (2015) estimated seismic hazard of Patna in Bihar considering the region-specific seismotectonic parameters, maximum moment magnitude and ground motion prediction equation. Kumar et al. (2013a, b) documented seismic hazard studies in terms of peak ground acceleration for the Dehradun and Lucknow cities which are situated in the Himalayan foothills. National Disaster Management Authority (NDMA 2010) developed the probabilistic seismic hazard map for various parts of India. Most of the earlier published seismic hazard maps were developed for PGA values based on old attenuation relationships. No such studies are currently available for the Sitamarhi region. In this paper, seismic hazard analysis of Sitamarhi region has been attempted by PSHA using three different attenuations relationships, i.e., Jain et al. (2000), Boore et al. (2014) and Bajaj and Anbazhagan (2019). The Gutenberg-Richter recurrence law (Gutenberg and Richter 1956) parameters ‘a’ and ‘b’ have been estimated using the seismic data recorded within 500Km radius of Sitamarhi. The major aim of this paper is to document a comprehensive PSHA for the Sitamarhi region. This PSHA study incorporates not only PGA but also 5%-damped spectral accelerations (SA) at six periods (0.2, 0.5, 1, 2, 3, and 5s), so that the uniform hazard spectrum for Sitamarhi can be generated. Based on the PSHA, the bedrock PGA values at Sitamarhi with 2% and 10% exceedance probability in 50 years are 0.89 g and 0.61 g, respectively.

2. Geology and Seismotectonics of the Study Area

Bihar is one of the seismically active regions in India due to the proximity of the region with seismically active Himalayan region. India has been divided into four seismic zones (i.e., Zones II, III, IV and V) and these zones face higher risk of seismic activities with increasing zone numbers (IS 1893-2016). As per IS 1893-2016, part 1, 15.2% area of Bihar state is in zone V, 63.7% area is in zone IV, and 21.1% area is in zone III (Fig. 1b),

148 respectively. The area considered in this study has a 500 km radius with the centre at Sitamarhi (latitudes
149 26.6°N longitudes 85.48°E). As per geographical perspective, Eurasian and Indian tectonic plates colliding in
150 the north side of the Sitamarhi which create high seismic activity in the region. This collision formed the
151 Tibetan plateau and the Himalayan mountain range. As the India plate is drifting towards north-east at 5 cm/year
152 (2 inches/year) and the Eurasian plate moves to the northward direction at a rate of 2 cm/year (0.8 inches/year),
153 Therefore, India is considered as the one of the fastest drifting continents in the world (Kolathayar et al. 2012).
154 This causes deformation in both plates and Indian plate undergoing compression at a rate of 4 cm/year (1.6
155 inches/year). To perform the seismic hazard analysis, seismic features like faults, shear zones and lineaments
156 along with earthquakes (M_w > 4.0) are the most important parameters. North Bihar region lies near the
157 seismically active Himalayan belt and on the deep deposits of the Indo-Gangetic basin. It is also surrounded by
158 various active faults (Dasgupta et al. 1987) like Main frontal thrust (MFT), East Patna fault (EPF), West Patna
159 fault (WPF), Sitamarhi fault (SIF), Munger Saharsa Ridge fault (MSRF) etc. as shown in Fig. 2 and Table 1.
160 The East Patna fault (EPF) is most active among all these faults (Anbazghan et al. 2015). The interaction
161 between East Patna Fault (EPF) and Himalayan Frontal Thrust (HFT) has led to a number of earthquakes in the
162 past (Bhangar 1991).

163 The Sitamarhi has suffered numerous natural disasters including earthquakes. The frequency of seismic
164 events related to the above-mentioned faults is considerably high. Historic earthquakes such as Bihar-Nepal
165 earthquakes in 1934 and 1988; Nepal earthquake in 2015 and also many other earthquakes have caused
166 significant economic losses as well as the loss of lives in the Sitamarhi region. In Bihar-Nepal earthquake of
167 1934 and 1988, large fissures were formed, with many places suffered tilting and sinking of building
168 foundations. The region was destroyed by the 1934 Bihar-Nepal earthquake due to extensive liquefaction. The
169 whole of Sitamarhi district was nearly destroyed; not a single building was left unscathed. Large fissure of 73.2
170 m long, 7.5 m wide and 1m deep filled with sand had formed at Sitamarhi (Richter 1957). The most of the part
171 of Sitamarhi district lies in seismic zone 5 with a zone factor of 0.36 (IS 1893:2016). The sites have soft
172 sediment and high groundwater level, which creates an increased risk of liquefaction. Therefore, the ground
173 motion parameters need to be estimated considering local geology, lithological and hydrological consideration
174 (Verma et al. 2014).

175 **3. Earthquake Catalogue and Processing of Earthquake Data**

176 Previous earthquakes may provide some important information about the seismicity of the study area. For
177 collecting the earthquake source data, Sitamarhi (26.59° N, 85.50° E) has been considered as the center of the

study area with a radius of 500 km. A total of 62 linear seismotectonic sources and source to site distances (as shown in Table 2) have been identified from the Seismotectonic Atlas of India (GIS 2000). The closest distance (r_{min}) and longest distance (r_{max}) of different seismotectonic faults have been measure using ArcGIS (ArcMap) software (Burnwal et al. 2017; Burman et al. 2020). Several earthquake records are compiled from various literatures and websites such as the United States geological survey (USGS), National center of seismology, Strong motion virtual data center, Indian Meteorological Department (IMD) and Geological Survey of India. The seismic events used in this study occurred between 1900 and November 2020 with a moment magnitude (M_w) varying between 4 and 8.3. A total of 1098 main shock events have been collected, which consists of the date, time, latitude and longitude of the epicentre, focal depth and magnitude of earthquakes. These collected data were reported in different earthquake magnitude scale (i.e., moment magnitude (M_w), surface-wave magnitude (M_S), and body wave magnitude (M_b)). In order to maintain consistency, it is essential to convert all the different magnitudes to a single magnitude (e.g., moment magnitude (M_w)). The numerous researchers developed different empirical relationship for the conversion of magnitudes (Stromeyer et al. 2004; Castellaro et al. 2006; Bormann et al. 2007; Thingbaijam et al. 2008; Scordilis 2006; Storchak et al. 2013). Storchak et al. (2013) proposed magnitude conversion relationships has been used to convert M_S and M_B to M_w as mentioned below:

$$M_w = \begin{cases} 0.67M_s + 2.13 & M_s \le 6.47 \\ 1.10M_s - 0.67 & M_s > 6.74 \end{cases} \quad (1)$$

$$M_w = 1.38M_b - 1.79 \quad (2)$$

After converting all earthquake records in Mw, earthquake catalogue has been rearranged based on the moment magnitude as shown in Table 3.

4. Seismic Hazard Analysis

Probabilistic seismic hazard analysis (PSHA) is the most commonly used approach to evaluate the seismic hazard parameters for any engineering project. PSHA is not only calculating for the worst-case ground motion intensity; it also considers all possible earthquake events and resulting ground motions. Cornell (1968) proposed the probabilistic seismic hazard method to account for various uncertainties. Algermissen et al. (1982) modified PSHA method to consider the probability of occurrence of a particular magnitude, and probability of hypocentral distance and ground motion exceeding a specific value. The major outcome from the PSHA is the hazard curve which shows ground motion parameters such as PGA or spectral acceleration (SA) as a function of the mean annual rate of exceedance. Hazard curves for all sources are obtained by considering various

combinations of magnitudes, hypocentral distances and the level of ground shaking. The overall hazard curve has been obtained after combining all individual hazard curves. PSHA offers a framework for identifying, quantifying and rationally combining these uncertainties to provide a more comprehensive picture of the seismic hazard. The procedures followed in this present study are briefly described in the following sub-sections:

4.1 Identification and Characterization of All Earthquake Sources

The first steps of this study involve the identification and characterization of all earthquake sources (fault, rupture, lineaments etc.) available in the study area. A total of 62 seismic sources have been identified within the 500 km radial distance of Sitamarhi. All considered sources have experienced an earthquake magnitude of 4 or greater than 4 in the past. After identification, all sources have been characterized for the distribution of earthquake magnitudes. All sources have a maximum potential magnitude (M_{max}) of the earthquake that cannot be exceeded. One third of the overall length of fault is generally taken as surface rupture length (L) of the fault which producing the maximum earthquake (Mark 1977). The M_{max} has been determined (as tabulated in Table 2) for each earthquake sources using the following relationships between M_{max} and L (Wells and Coppersmith 1994):

$$M_{w\max} = 5.16 + 1.62 \log_{10} L \quad \text{for strike slip fault} \tag{3}$$

$$M_{w\max} = 5.00 + 1.22 \log_{10} L \quad \text{for reverse fault} \tag{4}$$

$$M_{w\max} = 4.86 + 1.32 \log_{10} L \quad \text{for normal fault} \tag{5}$$

$$M_{w\max} = 5.08 + 1.16 \log_{10} L \quad \text{for all types of fault} \tag{6}$$

4.2 Seismicity Parameter ‘a’ and ‘b’

A recurrence relationship describes the average rate at which an earthquake of certain magnitude will be exceeded. A simple and most widely used relation for determining the seismicity of a source zone is Gutenberg-Richter recurrence law. It is assumed as exponential distribution of magnitude and is generally expressed as:

$$\log N(M) = a - bM \tag{7}$$

Here, N(M) is the number of earthquakes greater than or equal to M, the parameter ‘a’ describes the seismic activity, and ‘b’ describes a relative abundance of large to smaller shock whose value is close to 1 (Anbazhagan et al. 2009). A lower value of ‘b’ denoted the occurrence of larger percentage of higher magnitude earthquakes, and higher ‘b’ value means larger percentage of lower magnitude earthquake occurrence out of the total number of earthquakes. Another seismic parameter ‘a’ value represented general earthquake activity in the study area during the study period. The value of ‘a’ describes the no of earthquakes per year. These seismicity

parameters of a and b values are region specific. The range of 'b' value is 0.6 < b < 1.5 for various parts in India (NDMA 2010). The earthquakes of magnitude 4.0 or greater than 4.0 have been considered in the calculation of seismicity for the Sitamarhi region. The histogram in Fig. 3 shows the summary of earthquake events in the last twelve decades which has been used in the present study. From this data, seismicity parameter of a and b values are calculated from Magnitude vs. logarithmic function of a cumulative number of events per year (Fig. 4). A comparison of estimated a and b values of the present study with the nearby areas are shown in Table 4. The G-R relationship for the Sitamarhi region is expressed as:

$$\log N(M) = 4.36 - 0.85M \tag{8}$$

4.3 Source-to-site distance and magnitude probability distribution

The spatial uncertainty in source-to-site distance can be described by the probability density function (PDF). Source to site distance has been characterized by comparatively coarse histogram to restrict the number of computations engaged in the accessible instance. The difference between shortest and longest possible distance has been divided into ten divisions. The approximation to the source-to-site probability distribution for west Patna fault (WPF-SS-1) and Sitamarhi fault's (SIF) first segment are 0.3053 and 0.354, respectively. By dividing each source zone into a large (1000 in this study) number of segments of equal length, the distribution of source-to-site distance has been characterized. The normalized histogram of source-to-site distance for WPF-SS-1 and SIF are shown in Figs. 5a and b.

The bounded or doubly truncated Gutenberg-Richter recurrence law, between the magnitude M_0 and M_{max}, is used to compute the probability density function (PDF) of M. The minimum magnitude M_0 is considered as 4 in this study and M_{max} are different for different faults as mentioned above in sub-section 5.1. For each source zone, the bounded probability distribution of magnitude with a lower bound M_0, and an upper bound M_{max} can be expressed in terms of cumulative distribution function (CDF) as:

$$P\left[M < m \middle| m_0 < m < m_{\max}\right] = \int_{M=m_0}^{M=m_{\max}} f_M(m)dm \approx f_M\left(\frac{m_0 + m_{\max}}{2}\right)(m_{\max} - m_0) \tag{9}$$

where the PDF, $$f_M(m) = \frac{\beta \exp\left[-\beta\left(m - m_0\right)\right]}{1 - \exp\left[-\beta\left(m - m_0\right)\right]} \tag{10}$$

The normalized histogram of approximation to the magnitude probability distribution for the WPF-SS-1 and SIF in the study area are shown in Figs. 6a and b.

4.4 Ground motion prediction equation (GMPE):

Region-specific ground motion prediction equation (GMPE) played a crucial role in the macro-zonation and micro-zonation of any location. The GMPEs are usually obtained empirically by least square regression for a particular site using the site-specific strong motion data. However, some amount of randomness in the data is inevitable due to uncertainty in the mechanics of rupture, variability of sources, travel path and site conditions. However, very limited region-specific GMPEs are available for various parts of the India and the world for using it in seismic hazard assessment (NDMA 2010). At the same time, various researches working with Next Generation Attenuation (NGA) models for better prediction of ground shaking and designing the earthquake-resistant structure (Atkinson and Boore 2006; Campbell and Bozorgnia 2008; Wooddell and Abrahamson 2012; Boore et al. 2014). The proper selection of GMPE is one of the crucial steps in a seismic hazard analysis. For the present work, three GMPEs (Jain et al. 2000; Boore et al. 2014; Bajaj and Anbazhagan 2019) have been selected. Jain et al. (2000) proposed the attenuation relationship for the central Himalayan region based on strong motion accelerographs (SMA) and structural response recorder (SSR) to calculate PGA. The functional form of this GMPE is as follows:

$$\ln(PGA) = b_1 + b_2 M + b_3 R + b_4 \ln(R) \tag{11}$$

where, PGA is the peak ground acceleration in g, for central Himalayan earthquakes co-efficient $b_1 = -4.135$, $b_2 = 0.647$, $b_3 = -0.00142$, $b_4 = -0.753$ and standard deviation (σ) = 0.59. There are several GMPEs developed for similar tectonic conditions which can be also used for Himalayan region (Anbazhagan et al. 2015). One such GMPE is the one proposed by Boore et al. (2014). The functional form of the GMPE proposed by Boore et al. (2014) is as follows:

$$\ln Y = F_E(M, mech) + F_P(R_{JB}, M) + F_S(V_{S30}, R_{JB}, M) + \varepsilon_n \sigma(M, R_{JB}, V_{S30}) \tag{12}$$

Here, lnY is the natural logarithm of a vertical ground motion intensity measure (e.g., PGA, SA in g); F_E, F_p and F_S represent period-dependent functions for the source (E for event), path (P) and site (S) effects, respectively; ϵ_n is the fractional number of the standard deviations of a single predicted value of lnY away from the mean; and σ is the total standard deviation of the model. The M, $mech$, R_{JB} and V_{S30} are the predictor variables. And the parameter mech = 0, 1, 2 and 3 for unspecified, SF, NF and RF, respectively. Bajaj and Anbazhagan (2018) reported the suitability of various functional forms for the distance and magnitude scaling using the mixed-effect regression of residual calculated from the functional form given by NGA-West 2 project. Based on that, Bajaj and Anbazhagan (2019) proposed the GMPE for the Himalayan region as:

$$\ln(Y) = a_1 + a_2(M-6) + a_3(9-M)^2 + a_4 \ln R + a_m \ln R(M-6) + a_7 R + \sigma \tag{13}$$

where $\ln Y, M, R$ and σ are the logarithm of ground motion, magnitude, hypocentral distance and standard deviation; $a_1, a_2, a_3, a_4, a_m, a_7$ are the corresponding regressions co-efficient. The coefficient a_m is equal to a_5 when $M_w < 6.0$ and $R < 300$, else equal to a_6. The comparison between the above three GMPEs has been shown for a moment magnitude of 6.5 in Fig.7. The PGA values according to Bajaj and Anbazhagan (2019) are the maximum compared to other two GMPEs. The PGA values calculated according to Boore et al. (2014) are in the middle of that calculated from Jain et al. (2000) and Bajaj and Anbazhagan (2019) GMPE.

4.5 Temporal uncertainty

Usually, the sources will produce earthquake of different sizes up to the maximum earthquake, with smaller earthquakes occurring more frequently than larger ones. The temporal uncertainty or the occurrence of earthquakes in a seismic source is described by the Poisson's model. The probability distribution is defined in terms of the annual rate of exceeding the ground motion level z at the site under consideration ($v(z)$), due to all possible pairs of the magnitude (M) and epicentral distance (R) of the earthquake event expected around the site, considering its random nature (Anbazhagan et al. 2009). The probability of ground motion parameter at a given site, Z, will exceed a specified level, z, during a specified time, T is expressed as follows:

$$P(Z > z) = 1 - e^{v(z)T} \leq v(z)T \tag{14}$$

where, $v(z)$ is (mean annual rate of exceedance) the average frequency during the time period T at which the level of ground motion parameters, Z, exceed level z at a given site. The function $v(z)$ incorporates the uncertainty in time, size and location of future earthquakes and uncertainty in the level of ground motion they produce at the site. The functional form of $v(z)$ is as follows:

$$v(z) = \sum_{n=1}^{N} \left(N_n(m_o) \int_{m=m_0}^{m_u} f_n(m) \left[\int_{r=0}^{\infty} f_n(r|m)\, P(Z > z|m,r) dr \right] dm \right) \tag{15}$$

where, $N_n(m_o)$ is the earthquake frequency of seismic source n above a minimum magnitude m_o; $f_n(m)$ is the probability density function for the minimum magnitude m_o and maximum magnitude m_u; $f_n(r|m)$ is the conditional probability density function for the distance to earthquake rupture; and $P(Z > z|m, r)$ is the probability that given a magnitude 'm' earthquake at a distance 'r' from the site, the ground motion exceeds level z.

5. Result and discussion

The hazard curve expresses the frequency of exceedance of various levels of ground motions as a function of ground motion parameter. The calculation of all the probabilities in terms of hazard curve defines the annual rate of exceedance versus corresponding ground motion. Hazard curves has been plotted for all the sources and

also the total hazard curve has been calculated based on all three GMPEs. The hazard curves plotted using the GMPE suggested by Boore et al. (2014) for all sources are shown in Fig. 8. It has been seen from the Fig. 8 that WPF-SS-1 is the most hazardous fault located at a hypocentral distance of 21.11 km, with s fault length of 63.04 km, and a maximum magnitude ($M_{W\,max}$) of 6.6. Similarly, SIF and WPF-SS-2 are also significantly hazardous faults for the Sitamarhi region. The total hazard curve for the study area has been generated by the summation of all the hazard curves obtained from all the sources. The three total hazard curves plotted using three different GMPEs are shown in Fig. 9. At PGA value 0.1 g the mean annual rate of exceedance is obtained as 0.34 using Jain et al. (2000), 0.95 using Boore et al. (2014), and 0.92 using Bajaj and Anbazhagan (2019) GMPEs, respectively. Corresponding return periods (reciprocal of the mean annual rate of exceedance) are 2.94 years, 1.05 years and 1.09 years accordingly. In Fig. 9, the value obtained using Boore et al. (2014) suggested GMPE are in between the values obtained using other two GMPEs. Therefore, total hazard curves at different periods for spectral acceleration (Sa) values have been calculated using Boore et al. (2014) GMPE. It can be inferred from the Fig. 9 using Boore et al. (2014) GMPE that, the mean annual rate of exceedance for 0.36 g at zero second period (PGA) is 0.029, which will give the return period 34.48 years. This indicates that PGA of 0.61 g has a 10 % probability of exceedance in 50 years at the Sitamarhi region. The cumulative hazard curves obtained for the Sitamarhi region for 5 % damped peak spectral acceleration at 0.2 s, 0.5 s, 1 s, 2 s, 3 s and 5 s period are shown in Fig. 10. Similar comparison as mentioned above indicates that the 5 % damped spectral acceleration of 0.36 g has a mean annual rate of exceedance of 0.259 for 0.2 s period, 0.033 for 0.5 s, 0.003 for 1 s, 0.00004 for 2 s periods, respectively. From these results it can be inferred that as the period of intesest changes, the corresponding return period also has been changed drastically. Initially, the return period decreases from 1 year (for PGA) to 4 years for 0.2 s and again increase to 30.3 years for 0.5 s, 294.11 years for 1 s and 25839.79 years for 2 s, respectively.

Another major end-product of a PSHA is the uniform hazard specta (UHS). The UHS are a spectral curve which shows the variation of spectral acceleration (SA) at different period for a same probability of exceedance. In the present study, UHS for Sitamarhi for 2 % and 10 % probabilities of exceedance in the 50 years have been shown in Fig. 11. The spectral acceleration at zero second period is called zero spectral acceleration (SA) or PGA for Sitamarhi. The PGA values of Sitamarhi region considering 2 % and 10 % probabilities of exceedance in the 50 years are 0.89 g and 0.61 g. Previously, Burnwal et al. (2016) documented the maximum PGA value for Sitamarhi region in their DSHA research as 0.262 g. A total of 62 faults has been identified and characterized in the region and their cumulative effects have been considered in this study. Two new GMPEs

applicable for Himalayan region have also been used in this study. The calculated PGA value from the present study is comparable and slightly higher than other published values, which may be attributed due to the consideration of updated seismicity and GMPEs in this study.

6. Conclusion

The article presents a seismic hazard analysis and site-specific design spectrum development for the Sitamarhi region, considering probabilistic approaches along with region-specific data. Based on the study, the following observation have been drawn from this study:

- The seismic parameter has been evaluated using the seismic data collected over a radius of 500 km, and 62 seismotectonic linear sources have been identified and characterised. The maximum earthquake magnitude was estimated by Wells and Coppersmith (1994) equation for all faults and the overall maximum magnitude has been found as 8 for MCT.
- The seismicity parameter of a and b were estimated from the Gutenberg-Richter (G-R) relationship considering historic moment magnitude data as 4.36 and 0.85, respectively. These values are in agreement with the earlier reported results from the nearby regions.
- Hazard curves are generated using three regions specific GMPEs (Boore et al. 2014; Jain et al. 2000; and Bajaj and Anbazhagan 2019). A mean total hazard curve (black curve with star marker in Fig. 9) has been presented considering equal weightage assigned to all three GMPEs used in the study. Different period hazard curves (Fig. 10) also developed for the period of 0.2 s, 0.5 s, 1 s, 2 s, 3 s and 5 s using the GMPE proposed by Boore et al. (2014).
- Uniform hazard spectrum (Fig. 11) for the 2 % and 10 % probability of exceedance in 50 years has been presented for the region which is situated at zone V as per the Indian seismic zonation map.
- The present result is more region-specific and advanced than the previous studies and can be used further for microzonation work of Sitamarhi district. The seismic hazard values given in this paper are based on a V_{s30} value of 1500 m/s. These presented curves in this study may alter when site-specific soil properties will be considered.

Declaration

Acknowledgements

The author(s) would like to greatly acknowledge to IIT Patna and Department of Higher Education (Govt. of India) for providing the funding for present work to carry out the doctoral research of first author for which no specific grant number has been allotted.

Conflict of interest

The authors declare that they have no known competing financial interests or personal relationships that can have appeared to influence the work reported in this paper.

References

1. Algermissen ST, Perkins DM, Thenhaus PC, Hanson SL, Bender BL (1982) Probabilistic estimates of maximum acceleration and velocity in rock in the contiguous United States (No. 82–1033), USGS. https://doi.org/10.3133/ofr821033.
2. Anbazhagan P, Vinod JS, Sitharam TG (2009) Probabilistic seismic hazard analysis for Bangalore. Natural Hazards 48(2), 145-166. https://doi.org/10.1007/s11069-008-9253-3.
3. Anbazhagan P, Bajaj K, Patel S (2015) Seismic hazard maps and spectrum for Patna considering region-specific seismotectonic parameters. Natural Hazards 78(2), 1163-1195. https://doi.org/10.1007/s11069-015-1764-0.
4. Anbazhagan P, Bajaj K, Dutta N, Moustafa SS, Al-Arifi NS (2017) Region-specific deterministic and probabilistic seismic hazard analysis of Kanpur city. Journal of Earth System Science 126(1), 12. https://doi.org/10.1007/s12040-016-0779-6.
5. Anbazhagan P, Bajaj K, Matharu K, Moustafa SS, Al-Arifi NS (2019) Probabilistic seismic hazard analysis using the logic tree approach–Patna district (India). Natural Hazards and Earth System Sciences 19(10), 2097-2115. https://doi.org/10.5194/nhess-19-2097-2019.
6. Atkinson GM, Boore DM (2006) Earthquake ground-motion prediction equations for eastern North America. Bulletin of the seismological society of America 96(6), 2181-2205. https://doi.org/10.1785/0120050245.
7. Bajaj K, Anbazhagan P (2018) Determination of GMPE functional form for an active region with limited strong motion data: application to the Himalayan region. Journal of Seismology 22(1), 161-185. https://doi.org/10.1007/s10950-017-9698-5.
8. Bajaj K, Anbazhagan P (2019) Regional stochastic GMPE with available recorded data for active region–Application to the Himalayan region. *Soil Dynamics and Earthquake Engineering 126*, 105825. https://doi.org/10.1016/j.soildyn.2019.105825.
9. Banghar AR (1991) Mechanism solution of Nepal-Bihar earthquake of August 20, 1988. J. Geol. Soc. India 37, 25-30.

10. Bommer JJ, Abrahamson NA (2006) Why do modern probabilistic seismic-hazard analyses often lead to increased hazard estimates? Bulletin of the Seismological Society of America 96(6), 1967-1977. https://doi.org/10.1785/0120060043.
11. Boore DM, Stewart JP, Seyhan E, Atkinson GM (2014) NGA-West2 equations for predicting PGA, PGV, and 5% damped PSA for shallow crustal earthquakes. Earthquake Spectra 30(3), 1057-1085. https://doi.org/10.1193/070113EQS184M.
12. Bormann P, Liu R, Ren X, Gutdeutsch R, Kaiser D, Castellaro S (2007) Chinese national network magnitudes, their relation to NEIC magnitudes, and recommendations for new IASPEI magnitude standards. Bulletin of the Seismological Society of America, 97(1B), 114-127. https://doi.org/10.1785/0120060078.
13. Burman A, Gautam R, Maity D (2020) DSHA Based Estimation of Peak Ground Acceleration for Madhubani and Supaul Districts Near Bihar–Nepal Region. Geotechnical and Geological Engineering, 38(2), 1255-1275. https://doi.org/10.1007/s10706-019-01086-7.
14. Burnwal ML, Burman A, Samui P, Maity D (2017) Deterministic strong ground motion study for the Sitamarhi area near Bihar–Nepal region. Natural Hazards 87(1), 237-254. https://doi.org/10.1007/s11069-017-2761-2.
15. Campbell KW, Bozorgnia Y (2008) NGA ground motion model for the geometric mean horizontal component of PGA, PGV, PGD and 5% damped linear elastic response spectra for periods ranging from 0.01 to 10 s. Earthquake Spectra 24(1), 139-171. https://doi.org/10.1193/1.2857546.
16. Castellaro S, Mulargia F, Kagan YY (2006) Regression problems for magnitudes. Geophysical Journal International 165(3), 913-930. https://doi.org/10.1111/j.1365-246X.2006.02955.x.
17. Cornell CA (1968) Engineering seismic risk analysis. Bulletin of the seismological society of America, 58(5), 1583-1606.
18. Das S, Gupta ID, Gupta VK (2006) A probabilistic seismic hazard analysis of northeast India. Earthquake Spectra 22(1), 1-27. https://doi.org/10.1193/1.2163914.
19. Dasgupta S, Mukhopadhyay M, Nandy DR (1987) Active transverse features in the central portion of the Himalaya. Tectonophysics, 136 (3-4), 255-264. https://doi.org/10.1016/0040-1951(87)90028-X
20. GSI. (2000). Eastern Nepal Himalaya and Indo-Gangetic Plains of Bihar, in: Seismotectonic Atlas of India and Its Environs, Geological Survey of India, edited by: Narula, P. L., Acharyya, S. K., and Banerjee, J., Delhi, India, 26–27.

21. Gutenberg B, Richter CF (1956) Earthquake magnitude, intensity, energy, and acceleration: (Second paper). Bulletin of the seismological society of America, 46(2), 105-145.
22. IS 1893 (2016) Part 1: Indian standard criteria for earthquake resistant design of structure, sixth revision, Bureau of Indian Standards, New Delhi, 2016.
23. Jain SK, Roshan AD, Arlekar JN, Basu PC (2000) Empirical attenuation relationships for the Himalayan earthquakes based on Indian strong motion data. In Proceedings of the sixth international conference on seismic zonation (pp. 12-15).
24. Joshi A, Mohan K (2010) Expected peak ground acceleration in Uttarakhand Himalaya, India region from a deterministic hazard model. Natural hazards 52(2), 299-317. https://doi/org/10.1007/s11069-009-9373-4.
25. Joshi A, Patel RC (1997) Modelling of active lineaments for predicting a possible earthquake scenario around Dehradun, Garhwal Himalaya, India. Tectonophysics 283(1-4), 289-310. https://doi.org/10.1016/S0040-1951(97)00149-2.
26. Kolathayar S, Sitharam TG, Vipin KS (2012) Deterministic seismic hazard macrozonation of India. Journal of earth system science, 121(5), 1351-1364. https://doi.org/10.1007/s12040-012-0227-1.
27. Kumar M, Wason HR, Das R (2013a) Deterministic seismic hazard assessment of Dehradun city. In Proceedings of Indian geotechnical conference, December 22–24, 2013, Roorkee.
28. Kumar A, Anbazhagan P, Sitharam TG (2013b) Seismic hazard analysis of Lucknow considering local and active seismic gaps. Natural hazards 69(1), 327-350. https://doi.org/10.1007/s11069-013-0712-0.
29. Mark RK (1977) Application of linear statistical models of earthquake magnitude versus fault length in estimating maximum expectable earthquakes. Geology 5(8), 464-466. https://doi.org/10.1130/0091-7613(1977)5<464:AOLSMO>2.0.CO;2.
30. NDMA (2010) Development of probabilistic seismic hazard map of India; Technical Report by National Disaster Management Authority, Government of India.
31. Orozova IM, Suhadolc P (1999) A deterministic–probabilistic approach for seismic hazard assessment. Tectonophysics 312(2-4), 191-202. https://doi.org/10.1016/S0040-1951(99)00162-6.
32. Peruzza L, Rebez A, Slejko D, Bragato PL (2000) The Umbria–Marche case: some suggestions for the Italian seismic zonation. Soil Dynamics and Earthquake Engineering 20 (5-8), 361-371. https://doi.org/10.1016/S0267-7261(00)00084-1.

33. Ram TD, Guoxin W (2013) Probabilistic seismic hazard analysis in Nepal. Earthquake Engineering and Engineering Vibration 12(4), 577-586. https://doi.org/10.1007/s11803-013-0191-z.
34. Reiter L (1990) Earthquake hazard analysis: issues and insights. New York: Columbia University Press, Vol.22, No.3, p.254.
35. Richter CF (1957) Introduction to seismology. Eurasia publishing house, New Delhi, p 768.
36. Scordilis EM (2006) Empirical global relations converting M_S and M_b to moment magnitude. Journal of seismology 10(2), 225-236. https://doi.org/10.1007/s10950-006-9012-4.
37. Storchak DA, Giacomo DD, Bondár I, Engdahl ER, Harris J, Lee WHK, Villaseñor A, Bormann P (2013) Public release of the ISC-GEM global instrumental earthquake catalogue (1900–2009) Seismol Res Lett 84(5):810–815.
38. Stromeyer D, Grünthal G, Wahlström R (2004) Chi-square regression for seismic strength parameter relations, and their uncertainties, with applications to an Mw based earthquake catalogue for central, northern and north-western Europe. Journal of Seismology 8(1), 143-153. https://doi.org/10.1023/B:JOSE.0000009503.80673.51.
39. Thingbaijam KKS, Nath SK, Yadav A, Raj A, Walling MY, Mohanty WK (2008) Recent seismicity in northeast India and its adjoining region. Journal of Seismology 12(1), 107-123. https://doi.org/10.1007/s10950-007-9074-y.
40. Todorovska MI, Gupta ID, Gupta VK, Lee VW, Trifunac MD (1995) Selected topics in probabilistic seismic hazard analysis. Report CE, 95(08).
41. Trifunac MD (1990) A microzonation method based on uniform risk spectra. Soil Dynamics and Earthquake Engineering 9(1), 34-43. https://doi.org/10.1016/S0267-7261(09)90008-2.
42. Verma M, Singh RJ, Bansal BK (2014) Soft sediments and damage pattern: a few case studies from large Indian earthquakes vis-a-vis seismic risk evaluation. Natural hazards 74(3), 1829-1851. https://doi.org/10.1007/s11069-014-1283-4.
43. Wells DL, Coppersmith KJ (1994) New empirical relationships among magnitude, rupture length, rupture width, rupture area, and surface displacement. Bulletin of the seismological Society of America 84(4), 974-1002.
44. Du W, Pan TC (2020) Probabilistic seismic hazard assessment for Singapore. Natural Hazards, 103(3), 2883-2903. https://doi.org/10.1007/s11069-020-04107-4.

45. Wooddell KE, Abrahamson NA (2012) New earthquake classification scheme for mainshocks and aftershocks in the NGA-West2 ground motion prediction equations (GMPEs). In Proceedings, 15th World Conference on Earthquake Engineering, Lisbon, Portugal.

List of Figures:

List of Tables:

Figures

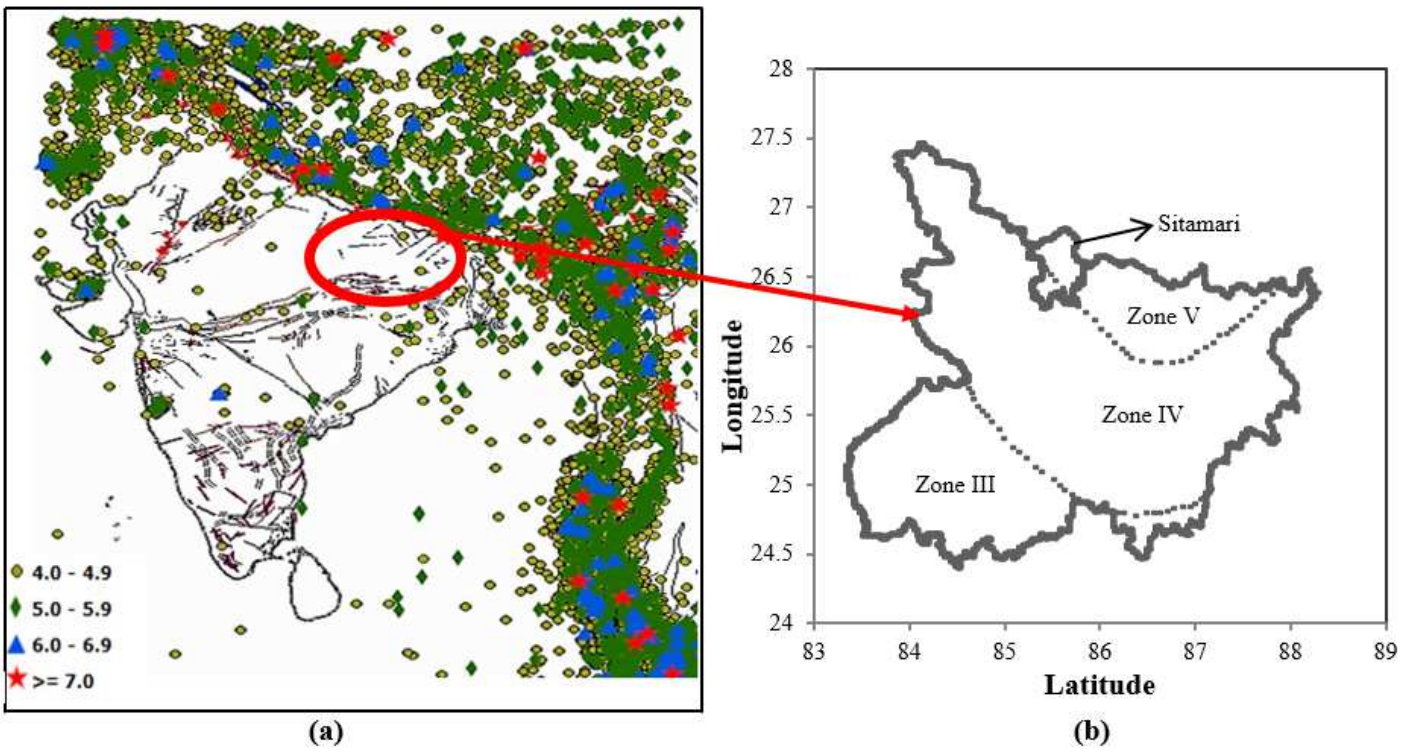

Figure 1

Earthquake event distribution map with study area (a) Plot of Earthquakes distribution (M>=4.0) from IMD catalogue from 1800 to 2015 (GSI). (b) Seismic zonation map of Bihar Note: The designations employed and the presentation of the material on this map do not imply the expression of any opinion whatsoever on the part of Research Square concerning the legal status of any country, territory, city or area or of its authorities, or concerning the delimitation of its frontiers or boundaries. This map has been provided by the authors.

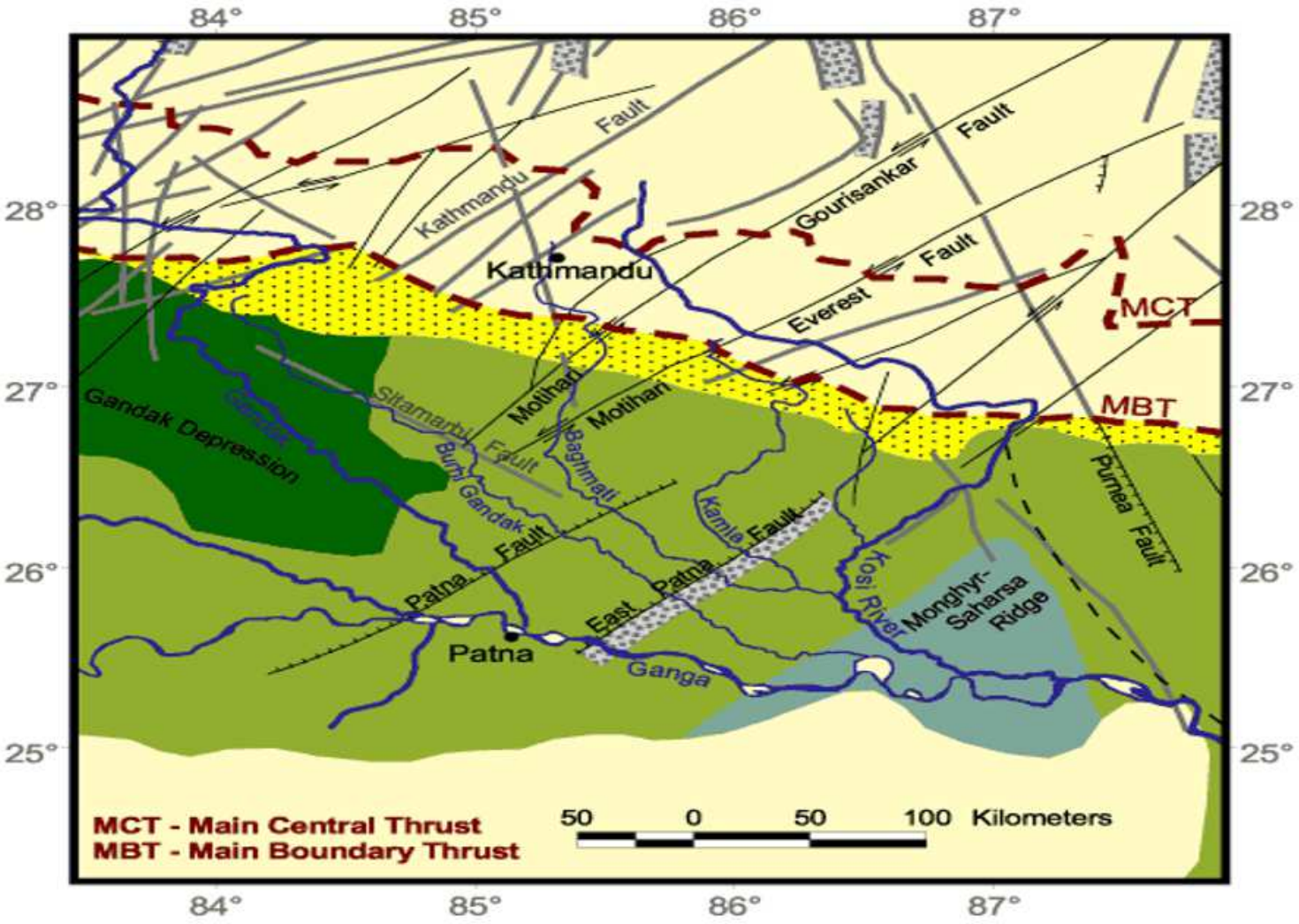

Figure 2

Seismic source map of the study area Note: The designations employed and the presentation of the material on this map do not imply the expression of any opinion whatsoever on the part of Research Square concerning the legal status of any country, territory, city or area or of its authorities, or concerning the delimitation of its frontiers or boundaries. This map has been provided by the authors.

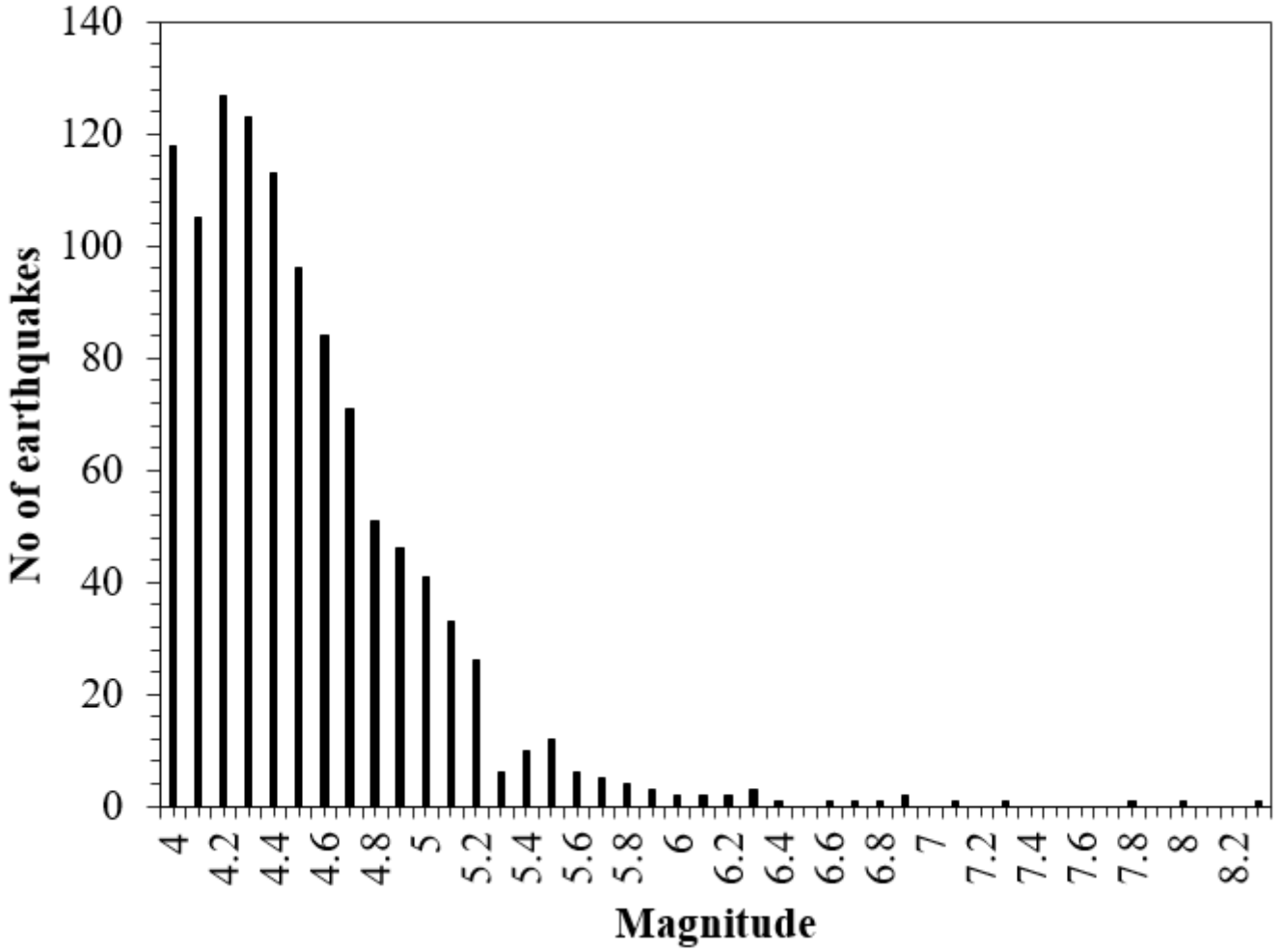

Figure 3

Chart showing the no. of earthquakes vs magnitude (4.0 and above) of earthquakes, from 1900 to 2020.

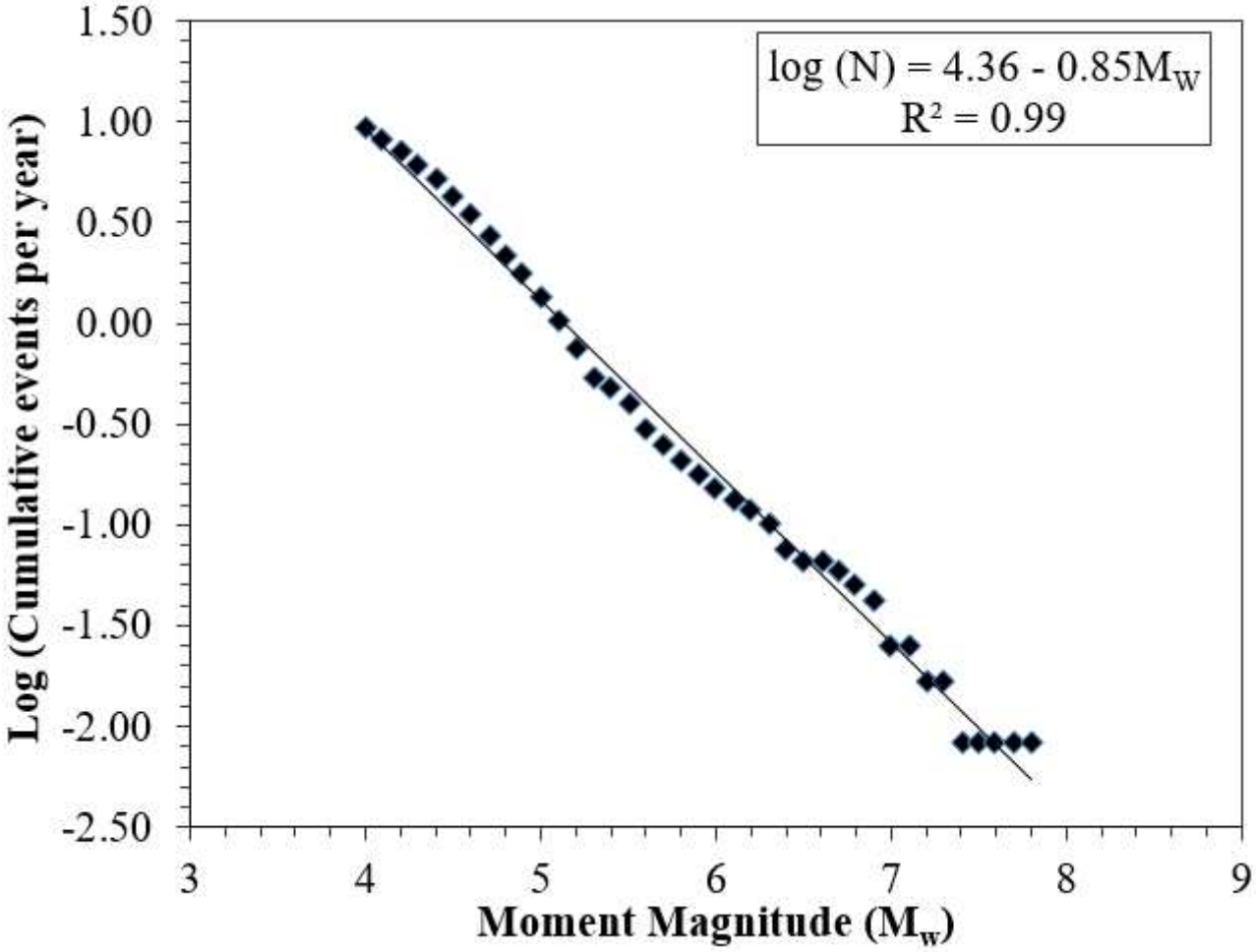

Figure 4

Gutenberg–Richter relation for the study region based on cumulative number of earthquakes per year

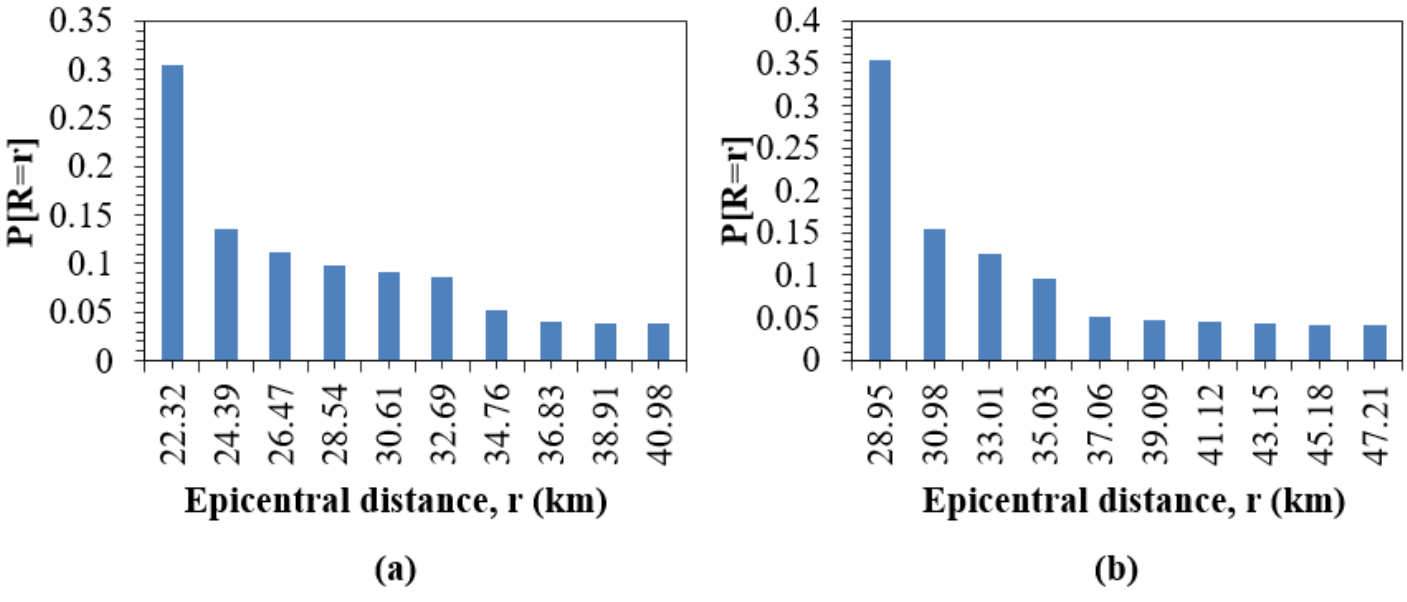

Figure 5

Approximations of source-to-site distance for (a) West Patna Fault and (b) Sitamarhi Fault

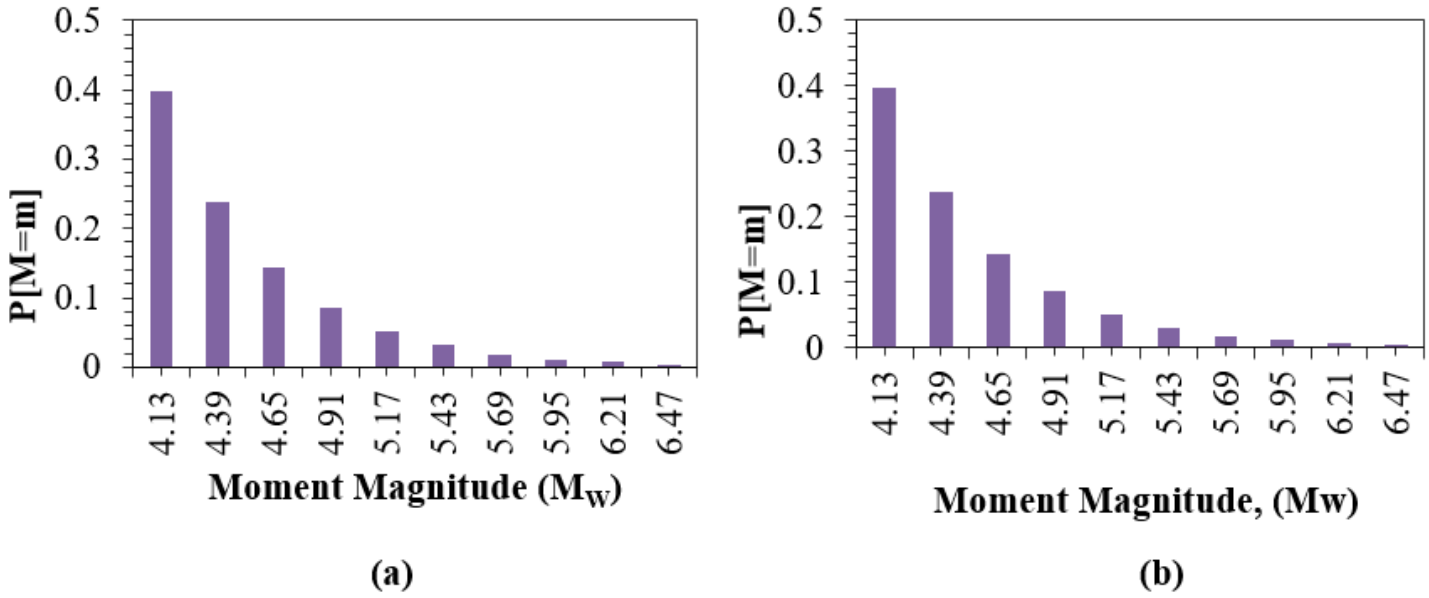

Figure 6

Approximations of magnitude probability distributions of (a) West Patna Fault and (b) Sitamarhi Fault

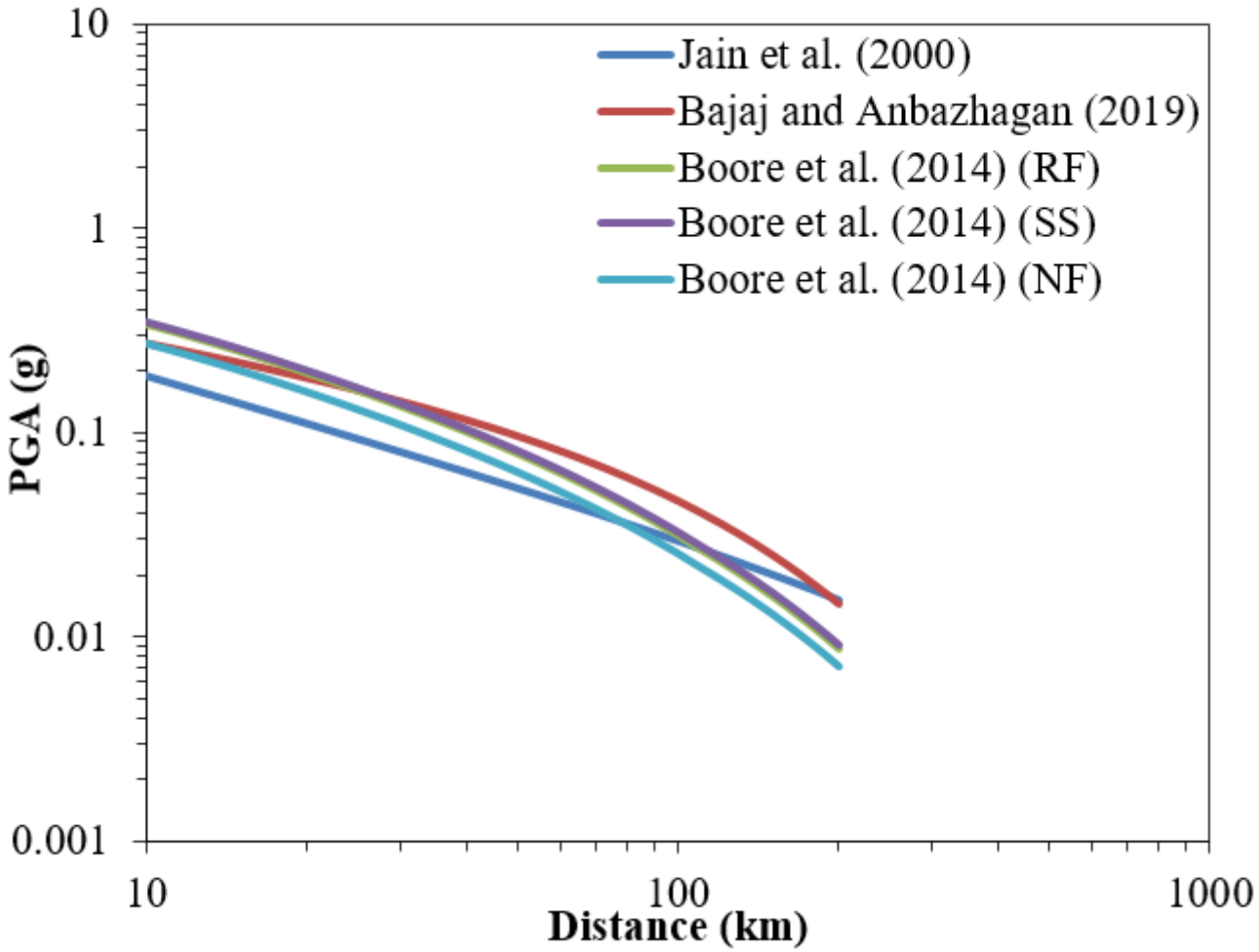

Figure 7

Comparison of PGA (g) with distance (km) at moment magnitude (MW) of 6.5 and Vs30 = 1500m/s (wherever applicable)

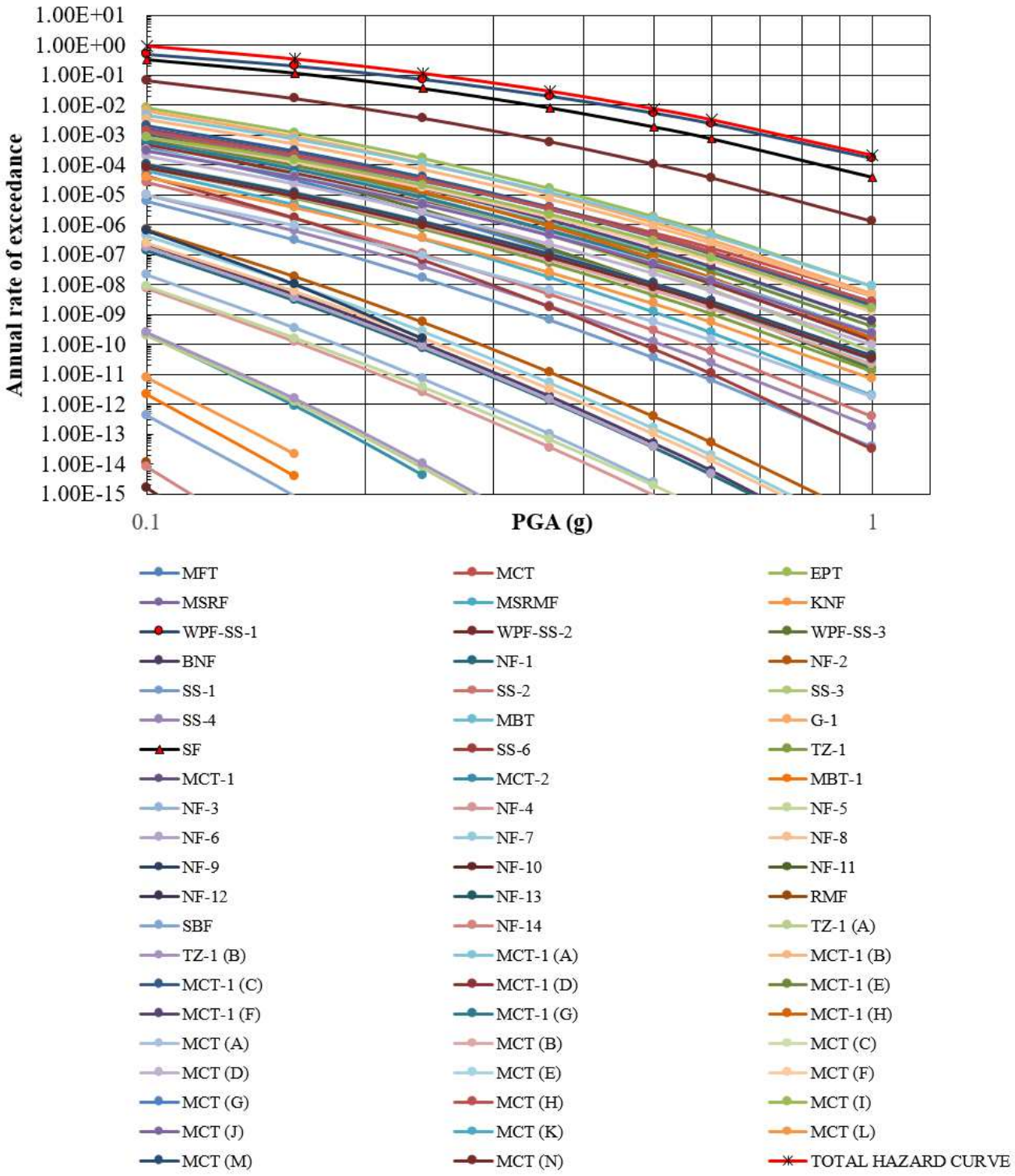

Figure 8

Seismic hazard curves developed based on Boore et al. 2014 for different sources and total seismic hazard curve for all sources

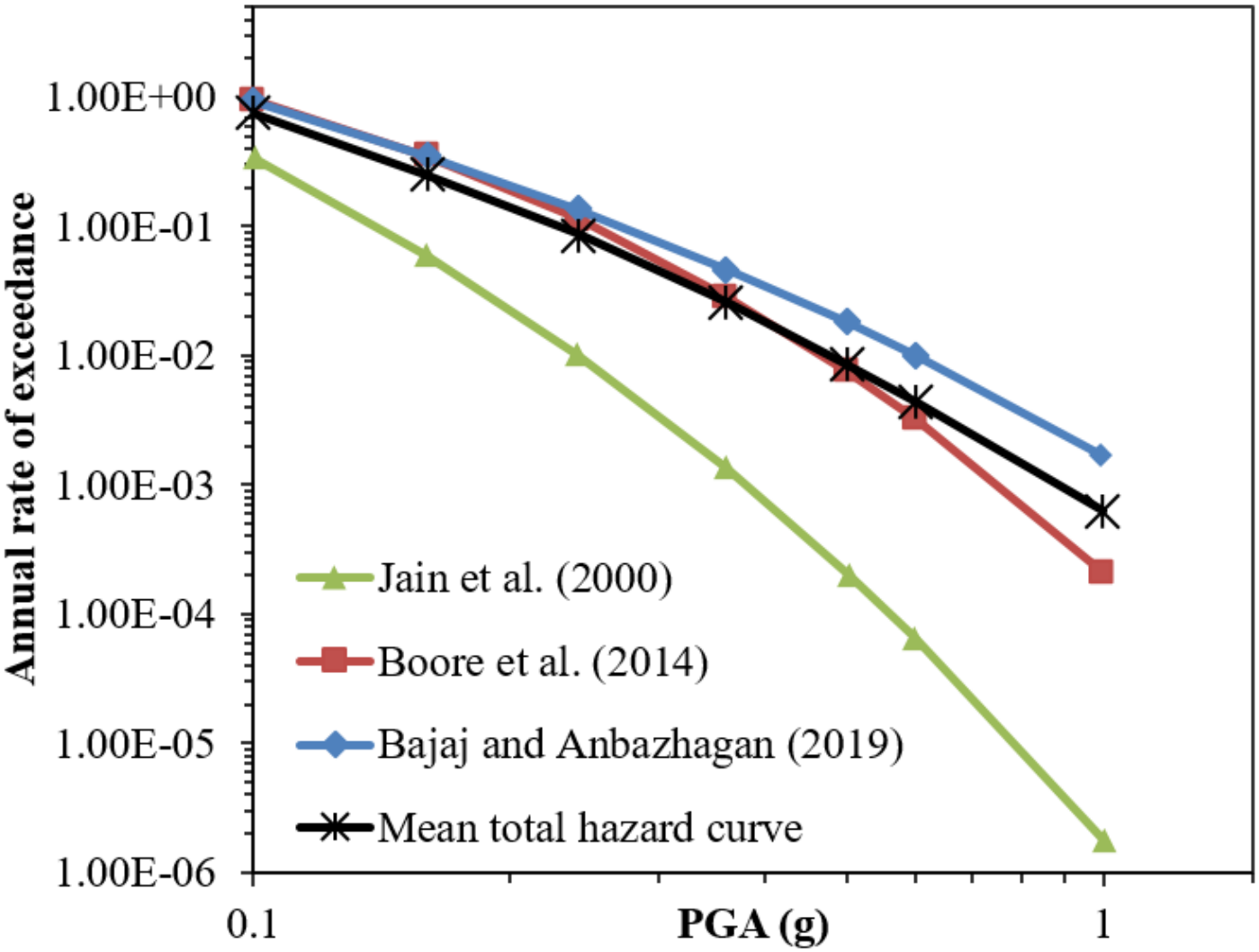

Figure 9

Total hazard curves calculated using three GMPEs for Sitamarhi

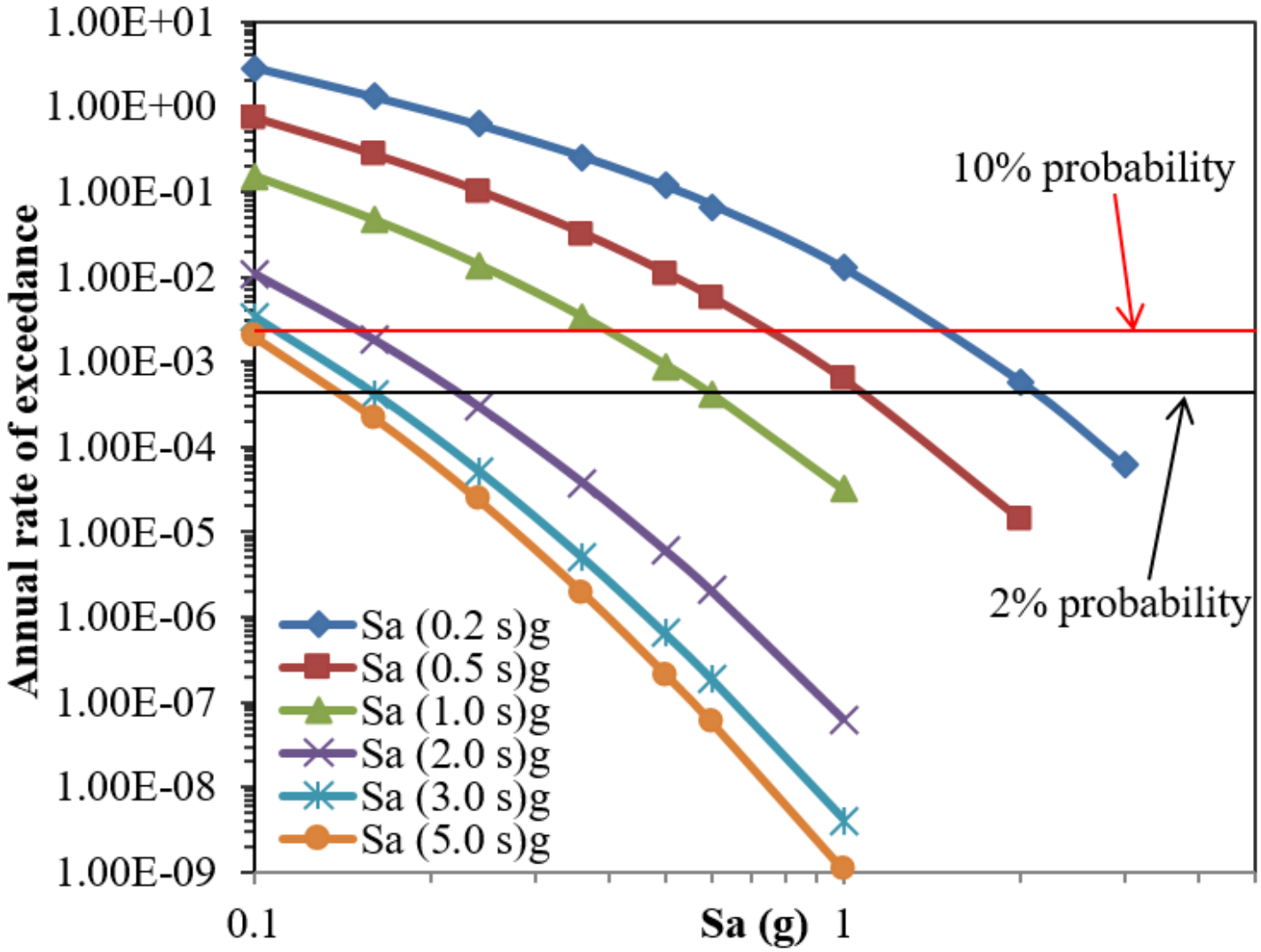

Figure 10

Total Hazard curves for Sitamarhi at different periods using classical approach and GMPE proposed by Boore et.al. (2014)

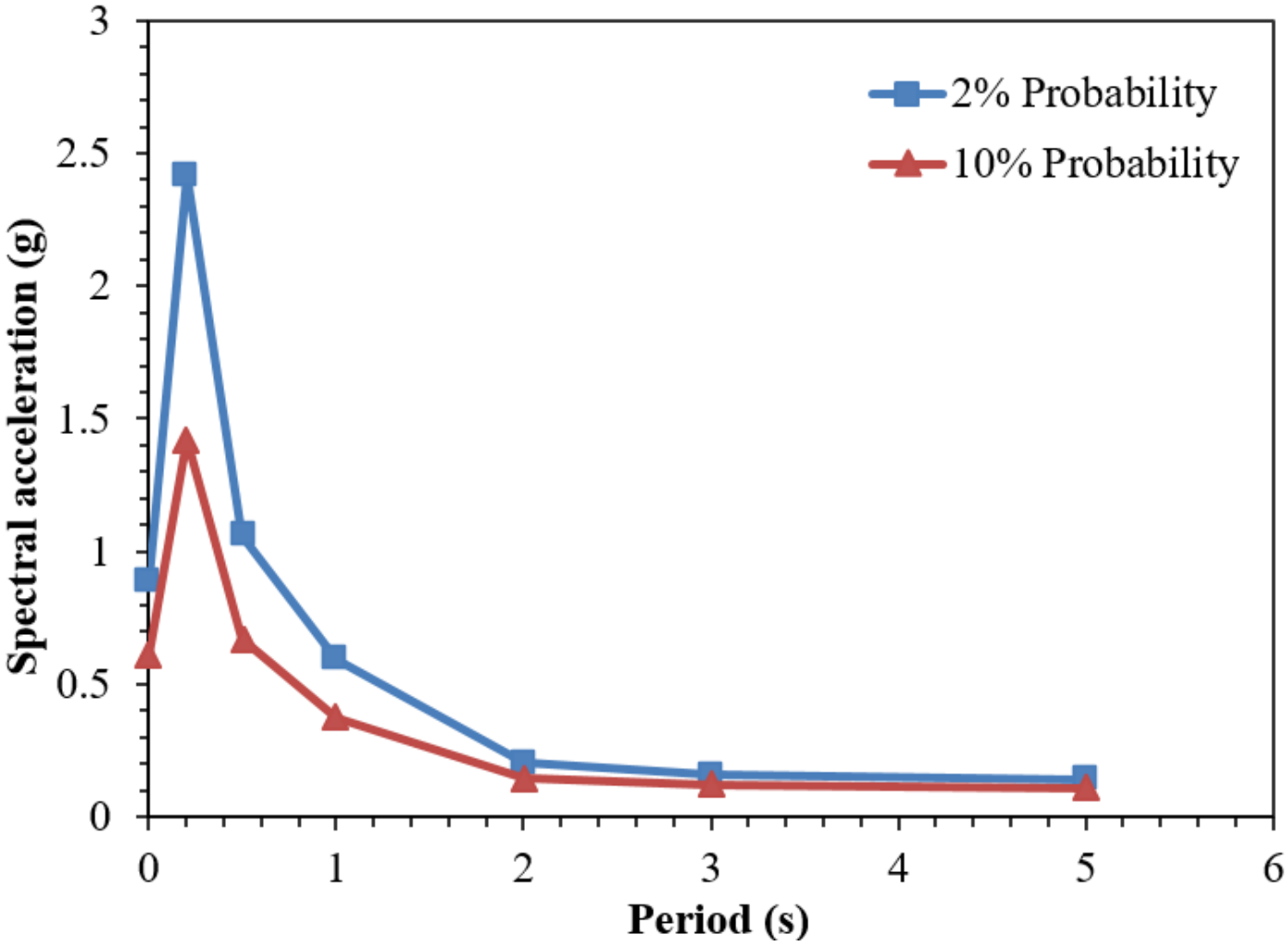

Figure 11

Uniform Hazard Spectrum (UHS) with 2% and 10% probability of exceedance in 50 years